

# Lacrimal Gland Microenvironment Changes After Obstruction of Lacrimal Gland Ducts

Xin He,<sup>1,2,4</sup> Shaopan Wang,<sup>2,4,5</sup> Huimin Sun,<sup>2,4</sup> Hui He,<sup>2,4</sup> Yalin Shi,<sup>1</sup> Yiming Wu,<sup>2,4</sup> Han Wu,<sup>2,4</sup> Zuguo Liu,<sup>2-4</sup> Jingyi Zhuang,<sup>1</sup> and Wei Li<sup>2-4</sup>

<sup>1</sup>Department of Ophthalmology, The First Affiliated Hospital of Xiamen University, School of Medicine, Xiamen University, Xiamen, Fujian, China

<sup>2</sup>Eye Institute of Xiamen University, School of Medicine, Xiamen University, Xiamen, Fujian, China

<sup>3</sup>Xiang'an Hospital of Xiamen University, School of Medicine, Xiamen University, Xiamen, Fujian, China

<sup>4</sup>Fujian Provincial Key Laboratory of Ophthalmology and Visual Science, Xiamen, Fujian, China

<sup>5</sup>Institute of Artificial Intelligence, Xiamen University, Xiamen, Fujian, China

Correspondence: Wei Li, Eye Institute of Xiamen University, Xiang'an Hospital of Xiamen University, School of Medicine, Xiamen University, Xiamen, Fujian, China, 4th Floor, 4221-122, South Xiang'an Rd, Xiamen, Fujian 361102, China; [wei1018@xmu.edu.cn](mailto:wei1018@xmu.edu.cn).

Jingyi Zhuang, Department of Ophthalmology, The First Affiliated Hospital of Xiamen University, School of Medicine, Xiamen University, Xiamen, Fujian, China, NO.55 Zhenhai Rd, Xiamen, Fujian 361003, China; [xmdyzhuangjy@sina.com](mailto:xmdyzhuangjy@sina.com).

**Received:** September 12, 2021

**Accepted:** February 24, 2022

**Published:** March 15, 2022

Citation: He X, Wang S, Sun H, et al. Lacrimal gland microenvironment changes after obstruction of lacrimal gland ducts. *Invest Ophthalmol Vis Sci.* 2022;63(3):14. <https://doi.org/10.1167/iovs.63.3.14>

**PURPOSE.** To investigate microenvironment changes of the lacrimal gland after obstruction of lacrimal gland ducts.

**METHODS.** The ducts of rat exorbital lacrimal gland were ligated by sutures for different durations. After that, the sutures in some animals were released, and they were observed for 21 days to evaluate the recovery of the lacrimal gland. Slit lamp and tear secretion test was performed to evaluate ocular surface and lacrimal gland function. The lacrimal gland and cornea were harvested and processed for hematoxylin and eosin staining, oil red O staining, LipidTOX staining, Masson staining, quantitative real time polymerase chain reaction, and immunofluorescence staining.

**RESULTS.** After the lacrimal gland ducts were blocked, tear secretion and the weight of the lacrimal gland were reduced. Incidence of corneal neovascularization increased after seven days. Intraglandular ducts dilated and acini destroyed. Long-term ligation induced fibrosis and lipid accumulation of the lacrimal glands. Inflammatory cell infiltrated and inflammatory factors upregulated. Proliferative and apoptotic cells increased. Structure of myoepithelial cells and basement membrane was destroyed. The p63 expression increased whereas Pax6 expression decreased. After suture release, tear secretion and structure of acini could recover in less than seven days after ligation, with a decrease in inflammatory cell infiltration and fibrosis relief. Apoptotic cells and proliferative cells increased at five days thereafter. The structure of the myoepithelial cells and basement membrane could not recover three days after ligation, and the number of mesenchymal cells increased in ligation after five to 14 days.

**CONCLUSIONS.** Blockage of the lacrimal gland ducts results in dystrophy of lacrimal gland acini cells, inflammation, and lipid accumulation of the lacrimal gland microenvironment. Long-term duct blockage will cause irreversible lacrimal gland failure.

**Keywords:** Lacrimal gland, microenvironment, duct obstruction

The lacrimal gland is an exocrine gland that is responsible for the aqueous tear including proteins and ions.<sup>1</sup> It plays an important role in maintaining the homeostasis of the healthy ocular surface microenvironment.<sup>2,3</sup> The lacrimal gland is composed of four different types of cells: acinar cell, duct cell, myoepithelial cell, and mesenchymal cell. In humans, there are about 12 tiny excretory ducts opening their orifice in the upper lateral fornix conjunctiva that drain aqueous tears into conjunctival sac.<sup>4</sup> The rat lacrimal gland contains exorbital and intraorbital lacrimal glands. The exorbital lacrimal gland is the main lacrimal gland located subcutaneously on the temporal side of the eye.<sup>5</sup> Adjacent to the exorbital lacrimal gland, the lacrimal gland contains six or more ducts. Farther toward the eye, it has three to five ducts.<sup>6</sup>

Many ocular surface diseases, such as Stevens-Johnson syndrome, cicatricial pemphigoid, severe infectious conjunc-

titis, ocular chemical burns, or thermal burns, could cause severe damage to the ocular surface tissues.<sup>7,8</sup> In addition to grievous injury of the conjunctiva, the orifice of lacrimal gland ducts are easily involved, and the ducts may be blocked at different stages of these diseases.<sup>9</sup> The fact is that little attention has been paid to protecting the lacrimal ducts or their orifices during severe ocular surface damage in clinics. At late stage of the diseases, even the orifices were reopened, the lacrimal gland usually could not regain its function to secrete aqueous tears. Thus lacrimal duct blockage or orifice closure became one of the most common reasons for severe aqueous tear-deficient dry eye resulted from these ocular surface diseases.

Currently, there is no knowledge about the time points that we can follow to save the structure and function of lacrimal gland if there is lacrimal duct or orifice obstruction

with severe ocular surface disease. Previous study has found that the lacrimal gland could be repaired by the progenitor cells after injury.<sup>10</sup> We may also get insight from the study of the parotid gland and sublingual gland that ligation of the duct could cause gland atrophy and dysfunction; nevertheless, the glands could regenerate through proliferation of the glandular cells after removal of the blockage on the appropriate occasion.<sup>11-14</sup> In a previous study that used three days' ligation of the rabbit lacrimal gland main excretory duct followed by reopening to investigate lacrimal gland tissue repair after short-term duct ligation-induced injury, it was found that the lacrimal gland stem/progenitor cell could be activated, and the lacrimal gland could recover normal structure and function.<sup>15</sup> Another study found that the mouse lacrimal gland could regenerate after seven days of duct ligation.<sup>16</sup> However, whether the recovery process could occur and the lacrimal gland is capable of regenerating after relatively long-term ductal blocking is still unknown.

In this study, we fabricate the rat lacrimal gland injury model with obstruction of the exorbital lacrimal gland ducts and observe the pathological changes during different time points after ligation and the recovery process. Our current study could mimic the occlusion of lacrimal gland ducts in clinical patients and provide evidence of timely treatment on release of the blocked duct.

## MATERIALS AND METHODS

### Materials

Anti-polymorphonuclear leukocyte (PMN) antibody (1:1200, 20R-PR020) was from Fitzgerald (Acton, MA, USA). Anti-CD68 (1:200, ab31630), anti-alpha smooth muscle actin ( $\alpha$ SMA, 1:200, ab184675), anti-p63 (1:200, ab124762), anti-Ki67 (1:400, ab16667), anti- $\beta$ -III tubulin (1:200, ab52623) and anti-vimentin (1:200, ab8978) antibodies were from Abcam (Cambridge, UK). Anti-laminin 5 antibody (1:200, sc-13587) was from Santa Cruz (Dallas, TX, USA). Anti-AQP5 antibody (1:100, A9927) was from Abclonal (Wuhan, China). Alexa Fluor 594-conjugated IgG (1:300, A11058, A21207) and Alexa Fluor 488-conjugated IgG (1:300 A11055, A21206) antibodies were from Life Technologies (Carlsbad, CA, USA). DAPI was from Vector (San Francisco, CA, USA).

### Rat Lacrimal Gland Ducts Obstruction Model

Sixty male SD rats (seven to eight weeks old, purchased from Shanghai SLAC laboratory animal center, Shanghai, China) were used in this study. All animals were kept in individual ventilated cages with standard environment throughout the study as follows: room temperature  $25^{\circ} \pm 1^{\circ}\text{C}$ , relative humidity  $60\% \pm 10\%$ , and alternating 12-hour light/dark cycles (8 AM to 8 PM). All experimental procedures were performed in accordance with the ARVO Statement for the Use of Animals in Ophthalmic and Vision Research, and the experimental protocol was approved by the experimental animal ethics committee of Xiamen University, Xiamen, China.

After induction of general anesthesia with pentobarbital sodium, the right exorbital lacrimal gland ducts were ligated by 5-0 nylon sutures as the ligation group, whereas the connective tissue around lacrimal gland was sutured as the sham operation group. The left exorbital lacrimal gland without operation was named as the control group.

For the ligation, sham operation, and control groups, the rats were killed by cervical dislocation at one, three, five, seven, 14, and 21 days after operation. For the release group, the sutures were removed at one, three, five, seven, 14, and 21 days after ligation or sham operation, and the animals were kept for 21 days before sacrifice (Fig. 1A). All animals were observed with slit lamp microscopy before sacrifice. The lacrimal glands from both sides were harvested for histologic study, immunostaining, and RNA extraction.

### Tear Secretion Measurement

Tear production was measured by the phenol red thread test using cotton threads (Zone-Quick; Yokota, Tokyo, Japan) at a similar time point (3 PM) before sacrifice in the standard environment. After induction of general anesthesia, the lower eyelid was pulled down slightly, and a 30 mm thread was placed on the palpebral conjunctiva for 15 seconds at a specified point approximately one third of the distance from the lateral canthus of the lower eyelid. The values indicated by the red color position of the aqueous front on the thread were recorded in millimeters.

### Slit Lamp Microscopy Evaluation and Corneal Fluorescein Staining

Ocular surface was observed by a slit lamp microscope (Kanghua Science & Technology Co., Ltd., Chongqing, China). Liquid sodium fluorescein 0.1% 2  $\mu\text{L}$  was dropped into the conjunctival sac. Then the rat eyelids were manually blinked three times. Excessive fluorescein sodium overflowing beyond the eyelids was rinsed with saline solution after the rat eyelids were closed. Corneal epithelial fluorescein staining was evaluated under the slit lamp microscope with a cobalt blue filter after 90 seconds.

### Immunofluorescent Staining

All immunofluorescent staining was performed on cryosections (6  $\mu\text{m}$  thickness) of the lacrimal gland and eyeballs. Sections were fixed in 4% paraformaldehyde for 15 minutes at room temperature. After being washed in phosphate-buffered saline solution (PBS), the sections were incubated in 0.2% Triton X-100 for 10 minutes. After being washed three times with PBS for five minutes each, all sections were incubated with 2% bovine serum albumin to block nonspecific staining for 60 minutes. Sections were then incubated with antibodies overnight at  $4^{\circ}\text{C}$ . After three washes with PBS for 10 minutes each, the sections were covered with Alexa Fluor 594-conjugated IgG or Alexa Fluor 488-conjugated IgG for 60 minutes at room temperature, followed by being washed three times with PBS for 10 minutes each. All sections were stained with DAPI and mounted and photographed with a laser confocal microscope (Olympus Fluoview 1000; Olympus, Tokyo, Japan).

### In Situ Terminal Deoxynucleotidyl Transferase dUTP Nick End Labeling (TUNEL) Assay

To measure the end-stage apoptosis, TUNEL staining on lacrimal gland was performed at different time points of

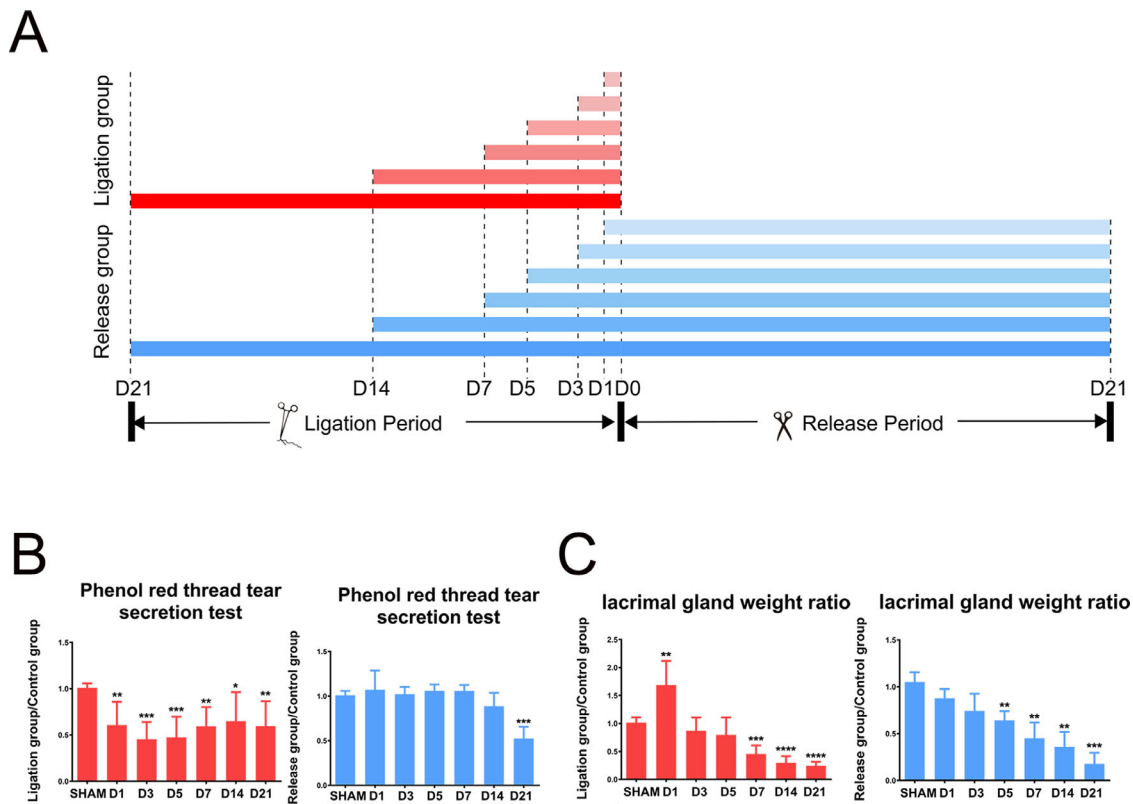


**FIGURE 1.** Tear secretion and lacrimal gland weight changed after lacrimal gland duct ligation and release. (A) Image showed pattern diagram of experiment. For the ligation group, the rats were sacrificed at one, three, five, seven, 14, and 21 days after operation. For the release group, the sutures were removed at one, three, five, seven, 14, and 21 days after ligation, and the animals were kept for 21 days before sacrifice. (B) Phenol red thread tear secretion test showed tear secretion after the ducts were ligated and the sutures were released. (C) The weight of lacrimal gland changed throughout the whole process after obstruction and unblockage ( $n = 5$ ;  $*P < 0.05$ ;  $**P < 0.01$ ,  $***P < 0.001$ ). The experiment was statistically analyzed using the *t*-test method. (B, C).

duct ligation. The frozen sections were incubated with 4% paraformaldehyde for twenty minutes, followed by three times PBS washed for five minutes each. Then all sections were covered with 20  $\mu\text{g}/\text{mL}$  proteinase K for 15 minutes at room temperature. After three washes with PBS for five minutes each, they were incubated with reagent mix (Dead-End Fluorometric TUNEL System G3250; Promega, Madison, WI, USA) at 37°C for one hour according to manufacturer's instructions. Then saline sodium citrate were used to terminate reaction for 15 minutes. Tissues were rinsed three times in PBS and counterstained with DAPI, mounted, and photographed with laser confocal microscope (Olympus Fluoview 1000).

### LipidTOX Staining

LipidTOX staining was used to observe neutral lipid distribution in lacrimal gland. Cryosections were fixed with 4% paraformaldehyde for 20 minutes, and sections were washed three times for five minutes using PBS after the fixative was discarded. We diluted the lipidTOX solution to  $\times 1$  with PBS. The solution was dropped on the specimen, discarded after 30 minutes staining, and washed three times with PBS for five minutes each. Slides were mounted with DAPI (Vector, CA, USA) and photographed with laser confocal microscope (Olympus Fluoview 1000).

### Oil Red O Staining

Oil red O staining was performed to observe the lipid accumulation of lacrimal gland as previously reported.<sup>17</sup> All cryosections were fixed with 4% paraformaldehyde for five minutes, followed by PBS rinsing for five minutes. Then tissues were incubated with 60% isopropanol for 20 seconds and stained for 15 minutes with 0.5% oil red O dissolved in isopropanol, followed by rinsing in PBS for five minutes. Sections were co-stained with hematoxylin and mounted with glycerin and observed under a light microscope (Zeiss Axio Lab.A1; Zeiss, Oberkochen, Germany).

### Masson Trichrome Staining

To investigate the distribution of collagen fiber, Masson trichrome staining kit (D026; Nanjing Jiancheng Bioengineering Institute, Nanjing, China) was applied on lacrimal gland tissues. In brief, paraffin sections were dewaxed before staining. Tissues were rinsed with double distilled water for two minutes at 37°C, followed by nuclear staining, cytoplasm staining, color separation, and counterstaining according to the manufacturer's instructions. After douching with pure ethyl alcohol, sections were mounted with mounting medium (H-5000; Vector Laboratories, Burlingame, CA, USA) and observed under a light microscope.

TABLE. Primer Sequences for the Real-Time PCR

Gene Name	Forward Primer	Reverse Primer
$\beta$ -actin	5'-CACCCGCGAGTACAACCTTC-3'	5'-CCCATACCCACCATCACACC-3'
P63	5'-CAGCACACGATCGAGACGTA-3'	5'-CGGGACTCCACAAGTCATT-3'
Pax6	5'-AGTTCTTCGCAACCTGGCTA-3'	5'-TTGGTGTTTTCTCCCTGTCC-3'
TNF $\alpha$	5'-TGCCTCAGCCTCTTCTCATT-3'	5'-GGGCTGTGCTACTCGAGTTTT-3'
IL1 $\beta$	5'-CCTCGTCTAAGTCACTCGC-3'	5'-GGCTGGTTCCTACTAGGCTTT-3'
TSG6	5'-GAAGCCAAGGCGGTATGTGA-3'	5'-TCAATGATGCCGGTTTTGCC-3'
Ki67	5'-CCTACAAGCAGCCTTCACGA-3'	5'-TCTGCTGCTGCTTCTCCTTC-3'
IL10	5'-CCTGGTAGAAGTGATGCCCC-3'	5'-TTGAGTGTCACGTAGGCTTCT-3'
$\alpha$ SMA	5'-AGAAGCCAGCCAGTCGCCATCA-3'	5'-AGCAAAGCCCGCCTTACAGAGCC-3'

### Quantitative Real Time Polymerase Chain Reaction (qRT-PCR)

Total RNA of lacrimal gland was extracted in TRIzol (Invitrogen, Carlsbad, CA, USA) and was reverse transcribed into cDNA by using ExScript RT Reagent kit (Takara Bio, Otsu, Shiga, Japan). Real-time PCR were performed with a StepOne Real-Time PCR detection system (Applied Biosystems, Germany) using a SYBR Premix Ex Taq Kit (Takara Bio) according to the manufacturer's instructions. The amplification program included an initial denaturation step at 95°C for 30 seconds, followed by denaturation at 95°C for 10 seconds, annealing at 60°C for 30 seconds, and extension at 60°C for 15 seconds for 40 cycles. The primers used to amplify specific gene products are shown in the Table. The results of the relative quantitative real-time PCR were analyzed by the comparative cycle method and normalized to  $\beta$ -actin as the reference gene.

### Image Analysis

For analysis of positive immunostaining ratio of lacrimal gland, images from Ki67 and TUNEL staining were processed by software Image J (National Institutes of Health, Bethesda, MD, USA). In brief, the fluorescence images were transferred into gray scale, images were adjusted threshold by software. Then we used the Watershed module to segment the staining into individual cells. Cell numbers were automatically counted by the Analyze Particles module. For analysis of immune-fluorescence intensity (PMN, CD68, AQP5,  $\beta$ -III tubulin), images were processed by Image J (National Institutes of Health). Briefly, after splitting channels of images, we used the auto-threshold from the software and measured the mean fluorescence intensity. All positive staining randomly selected at least three or more regions was analyzed by Image J software. All the samples were photographed with the same exposure time using a confocal laser scanning microscope (Fluoview 1000; Olympus). Each sample was recorded for at least three different areas.

### Statistical Analysis

Quantitative data are presented as means  $\pm$  SD. Independent Sample *t*-test and one-way analysis of variance (ANOVA) analysis of variance were applied to evaluate significance between groups. *P* < 0.05 was considered statistically significant. The statistical analysis was performed with Prism software version 8 (GraphPad Software, San Diego, CA, USA).

## RESULTS

### Tear Secretion Changes After Lacrimal Gland Duct Ligation and Release

There was progressive aqueous tear secretion decrease from day one to day five after lacrimal gland duct ligation. However, there was mild increase at day seven and maintained around half of the sham operation group until day 21. After duct ligation for different durations, the sutures of the lacrimal gland ducts were removed, and the animals were kept for recovering for 21 days. Aqueous tear secretion was then detected. We found that the tear secretion could recover to normal level if the ligation was released within seven days. After 14 days' blocking, the tear production could raise up slightly but could not recover to a normal level. After 21 days' obstruction, the tear secretion was about half of the sham operation after another 21 days' recover (Fig. 1B, Supplementary Fig. S1A).

Aquaporin 5 (AQP5) is a water channel protein involved in tear secretion.<sup>18,19</sup> Here, we observed AQP5 expression in the lacrimal gland. In the normal group, AQP5 was evenly distributed in acini and ducts. Although AQP5 positive expression was enhanced at the duct and downregulated in the acinus one day after ligation. A similar pattern was found at day seven and day 14. At 21 days, AQP5 expression was significantly reduced. In the release group, AQP5 was evenly distributed in acini and ducts within seven days, and AQP5 was only distributed in some acini and ducts after 14 days (Fig. 2A). Semiquantitative analysis of fluorescence intensity showed a gradual decrease of AQP5 expression after duct ligation and significant decrease in release group at day 14 and day 21 (Fig. 2C). The nerve regulates tear secretion in the lacrimal gland.<sup>20</sup> For nerve distribution, we observed a decrease of  $\beta$ -III tubulin expression after day 14 in ligation group and at day 21 in release group, indicating a decrease in nerve distribution at these time points (Figs. 2B, 2D). These results indicated that the tear secretion function of the acini was affected after one day of ligation, and the secretion function could not recover to normal stage if the lacrimal ducts were blocked for more than 14 days.

### Lacrimal Gland Weight Changes After Lacrimal Gland Duct Ligation and Release

Compared to the control group, the lacrimal gland weight of ligation group promptly increased to 1.32 folds after one day duct ligation, and it declined with fluctuation before five days. After seven days of blocking, the weight gradually decreased until 21 days. Release the ligation after one day or three days' blocking, the lacrimal gland weight showed

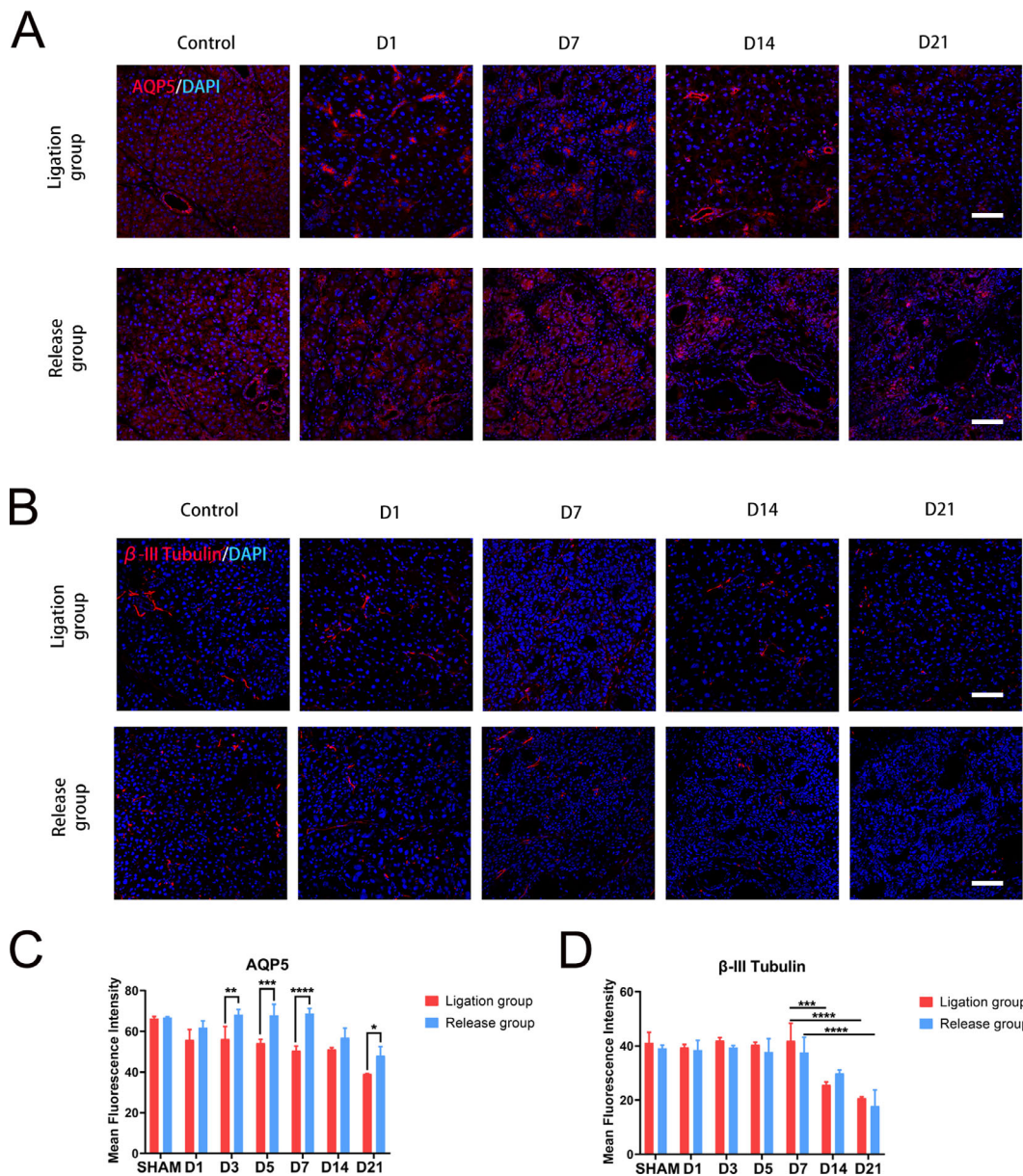


**FIGURE 2.** AQP5 and nerve distribution changes after lacrimal gland duct ligation and release. **(A)** Images showed immunofluorescence staining of AQP5 in lacrimal gland (Red: AQP5; Blue: DAPI). **(B)** Immunofluorescence staining of  $\beta$ -III tubulin indicates nerve distribution in lacrimal gland (Red:  $\beta$ -III tubulin; Blue: DAPI). Scale bars: 40  $\mu$ m **(C)** Graph showed mean fluorescence intensity of AQP5. **(D)** Graph shows mean fluorescence intensity of  $\beta$ -III tubulin (n = 5; \*P < 0.5, \*\*P < 0.01, \*\*\*P < 0.001 \*\*\*\*P < 0.0001). The experiment was statistically analyzed using the one-way ANOVA test method **(C, D)**.

minor decrease after recovering for 21 days. However, the weight of the lacrimal gland could not reverse if the ligation time was longer than three days (Fig. 1C, Supplementary Fig. S1B), indicating that there might be irreversible lacrimal gland dystrophy after duct ligation for more than three days.

### Ocular Surface Manifestations After Lacrimal Gland Duct Ligation and Release

We then observed ocular surface changes after lacrimal duct obstruction for different durations. The cornea remained transparent for seven days. After seven days occlusion of

the lacrimal ducts, neovascularization that grew into cornea stroma from nasal side could be observed (Fig. 3A). The morbidity of corneal neovascularization is about 25% after seven days' ligation and about 35% after 21 days' ligation (Fig. 3B). The corneal fluorescein sodium score showed that the degree of corneal epithelial defect gradually increased with time after duct ligation for three days. In the release group, the degree of corneal epithelial defects improved within 14 days. However, the corneal fluorescein sodium score increased significantly after 14 days (Fig. 3E). Hematoxylin and eosin (H&E) staining showed that the stroma of central cornea with blood vessel in-growth was incrasated and cell infiltration could be observed in these animals (Fig. 3C). PMN staining further confirmed that the infiltrated

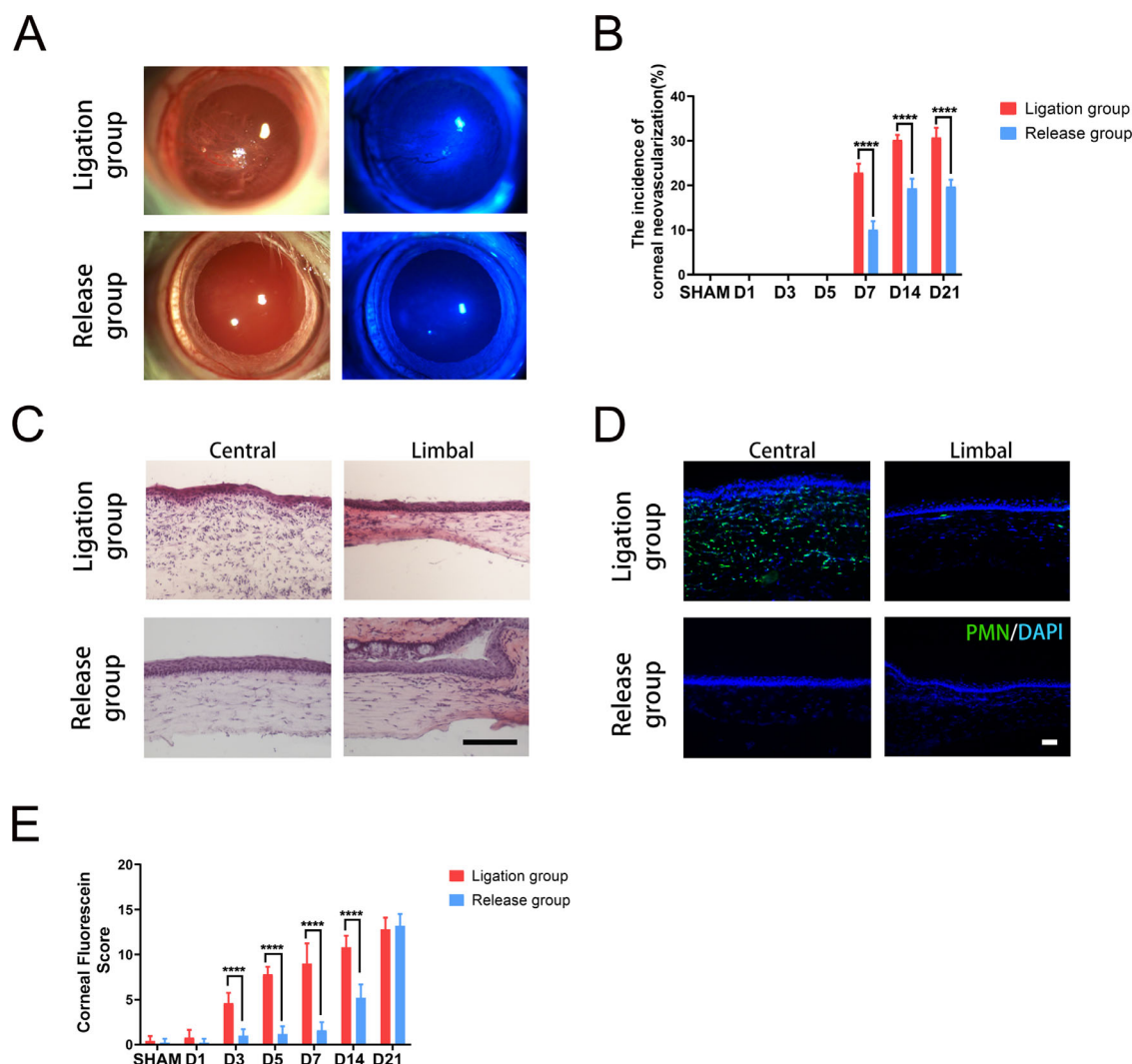


**FIGURE 3.** Ocular surface manifestations after lacrimal gland duct ligation and release. (A) Slit lamp and sodium fluorescein staining of cornea showed ocular surface changes after obstruction and after releasing sutures. (B) The incidence of corneal neovascularization after blocking the ducts and after re-opening the ducts. (C) H&E staining showed central and limbal cornea manifestation. *Scale bar:* 100  $\mu$ m. (D) Immunofluorescence staining of PMN showed polymorphonuclear leukocyte increased in ligation group and reduced significantly after releasing suture (*Green:* PMN; *Blue:* DAPI). *Scale bar:* 50  $\mu$ m. (E) Graph shows corneal fluorescein score of ligation group and release group ( $n = 5$ ;  $***P < 0.0001$ ). The experiment was statistically analyzed using the one-way ANOVA test method (B, E).

cells in the central corneal stroma contained numerous polymorphonuclear leukocytes (Fig. 3D).

### Lacrimal Gland Structure Changes After Lacrimal Ducts Blockage

To further investigate lacrimal gland changes after lacrimal duct ligation, we first performed H&E staining of the lacrimal gland tissues. There was obvious edema of acinar cells at one day after ligation of the ducts. After three days, many dilated ducts could be clearly observed, and the structure of the acinus became irregular, and the nuclei of some acinar cells also presented irregular shape. After five days ligation, some border of the acinus became obscure. There were many spindle-shaped nuclear cells infiltrated into stroma of the acinus after seven days ligation and became more prominent at day 14. Almost all the ducts became amplified obvi-

ously, and the normal acinar structure could not be found after 21 days ligation (Fig. 4A).

We then investigated the structure of the lacrimal gland after ligation release for 21 days after ligation for different durations. H&E staining showed that the structure of acinus and duct could be observed if the ligation was released before seven days, whereas the interspace between the acinus was enlarged as ligation time prolonged. However, the ducts kept dilating, and most of the acinus became severe atrophied, with numerous inflammatory cells infiltrated if the ligation was released after 14 days. Furthermore, there was no acinar structure left with numerous dilated ducts and infiltrated cells presented if the ligation was released after 21 days (Fig. 4). These results indicated that the structure of lacrimal gland could be severely damaged and could not recover to normal if the lacrimal ducts were blocked for more than seven days.

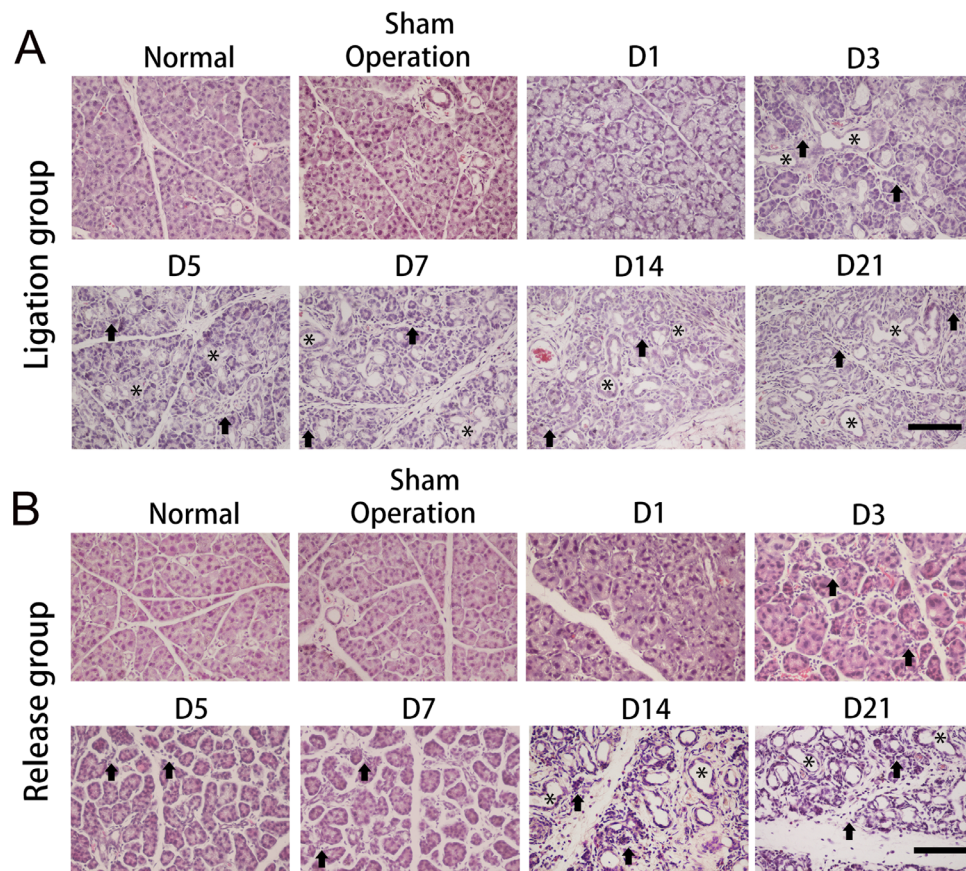


**FIGURE 4.** Lacrimal gland structure changes after lacrimal ducts blockage. (A) H&E staining showed ductal dilatation, cellular infiltration, and acinar atrophy of lacrimal gland in ligation group. (B) H&E staining showed that ductal dilatation and acinar atrophy improved before seven days in the release group. Scale bar: 100  $\mu$ m. Arrows indicate infiltrated cells; asterisks indicate dilated glandular ducts (n = 5).

### Fibrosis Process in the Lacrimal Gland After Lacrimal Ducts Blockage

We then performed Masson trichrome staining to determine fibrosis of the lacrimal gland. The results showed that positive staining gradually emerged after duct ligation for five days and the collagen fiber wrapped the ectatic ducts. However, the collagen inside the acinus gradually reduced. After 14 days' ligation, there was obvious fibrosis plaques surrounding blood vessels and major dilated ducts, and it became more severe after 21 days' ligation. However, the fibrosis was vivid in those release ligation performed after three days' blocking and became more evident as releasing time delayed from seven to 21 days (Fig. 5).

### Lipid Accumulation of Lacrimal Gland After Lacrimal Ducts Blockage

Lacrimal gland frozen sections were stained with lipid-TOX and oil red O solution to observe the neutral triglycerides. Very few small lipid dots were present in normal rat lacrimal gland in a diffused manner. One day after lacrimal duct obstruction, a few lipid droplet patches were visible around the acini. As time went on, the lipid droplet patches increased and combined into larger ones that aggregated around the acini or surrounding mesenchyme and dilated the ducts. In the ligation group at day seven and day 14, lipid deposition was diffusely distributed in the acini, whereas

clusters of lipids were observed at day 21. In the suture release group, there was a minor amount of lipid droplets at day one, whereas a large amount was observed in the partially dilated ducts and atrophic acini at seven days. The lipid droplets were deposited as clusters at 14 and 21 days. These results indicated that lacrimal duct obstruction could induce abnormal lipid accumulation in the lacrimal gland, and the lipid could retain if the ligation time is longer than seven days (Fig. 6).

### Inflammatory Cells Infiltration in Lacrimal Gland After Lacrimal Ducts Blockage

In the normal lacrimal gland, there were very few inflammatory cells.<sup>21</sup> PMN staining showed sporadic polymorphonuclear leukocytes in the normal rat lacrimal gland but increased from day one of lacrimal duct ligation and reached peak at day seven. The PMN-positive cells slightly decreased after 14 days (Figs. 7A, 7C). In the release group, the PMN-positive cells were much less than that of the ligation group from day one to day seven, although there was no obvious difference at days 14 and 21. To further evaluate the variety of infiltrated cells, we performed immunostaining of CD68 to assess the mononuclear macrophage. We found that macrophages gradually increased after five days and remained at a high level after day seven (Figs. 7B, 7D). In

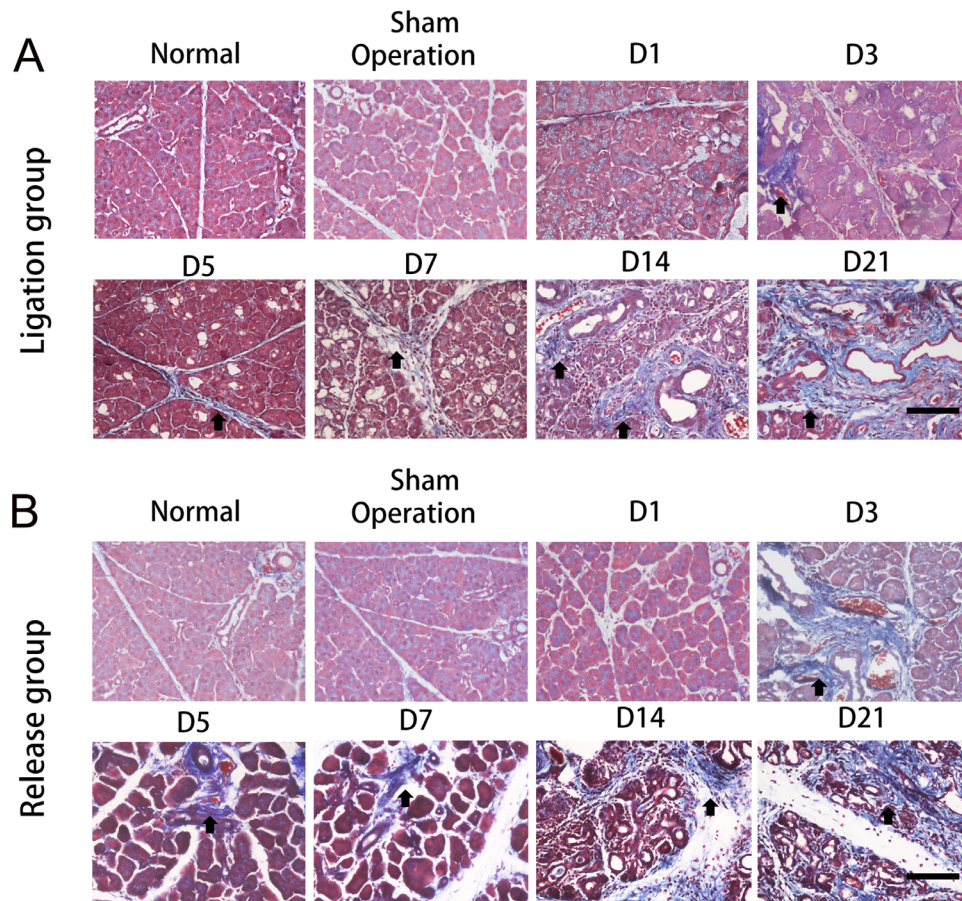


**FIGURE 5.** Fibrosis process in the lacrimal gland after lacrimal duct blockage. **(A)** Masson staining manifested fibrosis of the lacrimal gland starting at three days in the ligation group. **(B)** Masson staining showed that there was partial improvement in fibrosis within seven days in the release group. Arrows indicate collagen fibrosis in the lacrimal gland. Scale bar: 100  $\mu$ m, n = 5.

the release group, macrophage infiltration showed a similar pattern as the ligation group.

We further observed the expression of inflammatory cytokines in the lacrimal glands using qRT-PCR. The results showed that there was immediate dramatic increase of interleukin-1  $\beta$  (IL-1 $\beta$ ) at day one of lacrimal duct ligation, and IL-1 $\beta$  gene expression gradually decreased from day one to day 21 but was still higher than that of the control group at day 21. The expression of tumor necrosis factor- $\alpha$  (TNF- $\alpha$ ) gradually increased from day one to day 21. The expression of anti-inflammation factors, for instance, IL-10 showed similar pattern as IL-1 $\beta$ . TSG6 expression was obviously enhanced after three days, reached peak at day seven, and then gradually decreased. In the release group, qRT-PCR showed the expression of TNF- $\alpha$  and IL-1 $\beta$  gradually enhanced from day one to day 14. Interestingly, anti-inflammation factor IL-10 expression also gradually increased from day one to day 21. TSG6 expression increased dramatically if the release was performed at day three (Fig. 7E).

#### Cell Proliferation and Apoptosis in Lacrimal Gland After Obstruction of Lacrimal Gland Ducts

The apoptotic cells emerged in the acini of lacrimal gland, and they gradually increased after duct blocking for five

days. With releasing the obstruction of ducts, the apoptotic cells constantly appeared after five days and the amount is obviously higher than that of the obstruction group (Figs. 8A, 8C). Ki67 is a validated biomarker of cell proliferation. Ki67-positive cells gradually increased after three days of duct ligation and maintained a relatively high level from day seven to day 21. In the release group, Ki67-positive cells increased at day five and remained at a high level until day 21, whereas the percentage of Ki67-positive cells was less than that of obstruction group from day seven to day 21 (Figs. 8B, 8D).

#### Lacrimal Gland Myoepithelial Cell Changes After Obstruction of Lacrimal Gland Ducts

To observe the myoepithelial cell changes of the lacrimal gland,  $\alpha$ SMA and p63 immunofluorescence double staining were performed. In the normal group,  $\alpha$ SMA-positive cells were located in the basal site of the acinus and expressed  $\Delta$ Np63.<sup>22</sup> After the lacrimal gland ducts were blocked for one day, p63-positive staining was reduced. As time went on, more  $\alpha$ SMA-positive cells diminished and lost their normal morphology, especially after ligating the ducts for five days, and there was very weak  $\alpha$ SMA staining present from day seven to day 21. On the other hand, the expression of p63 increased from day three to day 21 (Fig. 9A). The qRT-PCR



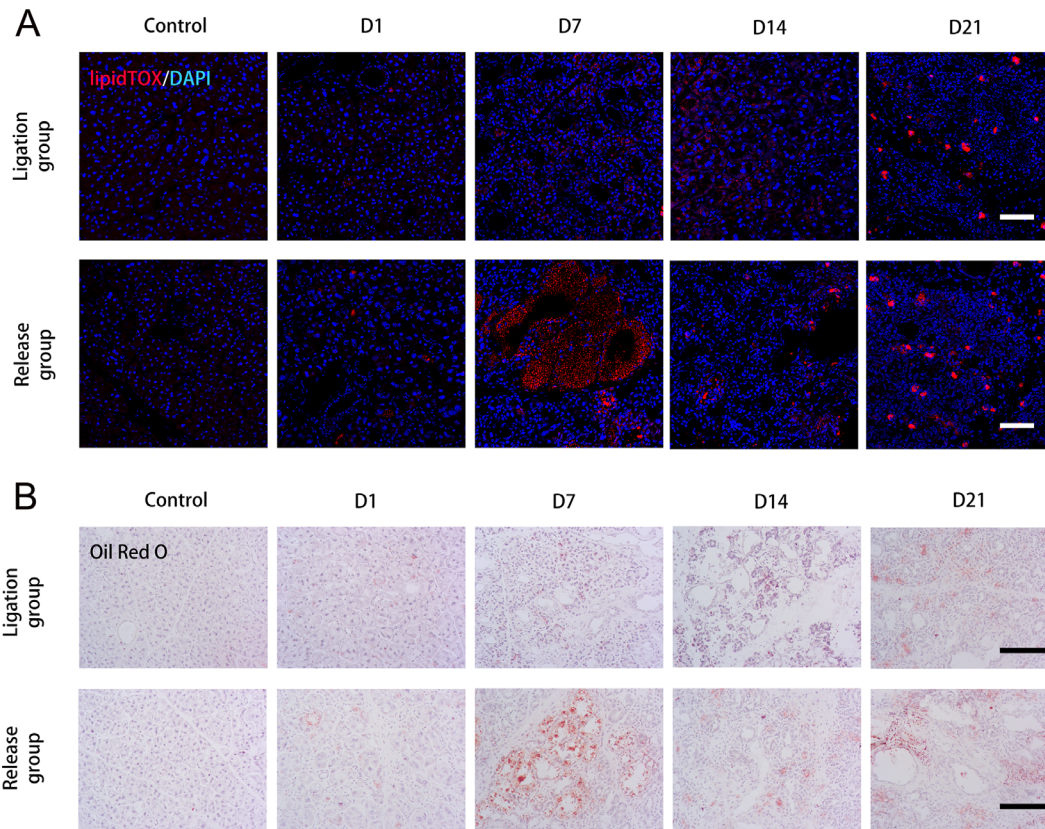


**FIGURE 6.** Lipid accumulation of lacrimal gland after lacrimal duct blockage. (A) LipidTOX staining showed neutral lipid distribution increased after seven days in the ligation group and the release group (Red: LipidTOX, Blue: DAPI). Scale bar: 40  $\mu$ m. (B) Oil red O staining showed neutral lipid accumulation in the lacrimal gland. Scale bar: 100  $\mu$ m, n = 5.

results confirmed that p63 expression gradually increased from day one to day 21 of duct ligation, whereas Pax6 expression decreased at day one and was maintained at a low level from day three to day 21,  $\alpha$ SMA gene expression dramatically decreased at day five and was maintained at a very low level from day five to day 21 (Fig. 9D). Moreover, we applied laminin 5 to investigate basement membrane alterations in the lacrimal gland acini. Laminin 5 is expressed at the basal side of the normal lacrimal gland acini. Although laminin 5 expression gradually decreased after seven days' ligation, and there were only sporadic positive expressions after 14 days of duct ligation (Fig. 9B). In addition, we used vimentin fluorescence staining to observe the changes of mesenchymal cells in the lacrimal gland. Within seven days of duct ligation, vimentin-positive cells could be seen scattered in the lacrimal gland. At 14 days, vimentin-positive cells were significantly increased and distributed in acini, ducts, and stroma. However, positive cells were significantly reduced at 21 days (Fig. 9C, Supplementary Fig. S2).

With release of the sutures, the morphology of the myoepithelial cells could recover if the release was performed within three days. However, the  $\alpha$ SMA-positive cells almost completely disappeared if the release was performed after five days, and there was no  $\alpha$ SMA recovery until 21 days (Fig. 9A). For the p63 expression, we found that the quantity of positive cells was augmented after five days and reached the top at seven days and then gradually decreased after 14 days (Fig. 9A). The qRT-PCR confirmed a similar p63 gene expression pattern as that of immunos-

taining (Fig. 9E). Pax6 gene expression showed a transient increase at day one but gradually reduced to a lower-than-normal level at days 14 and 21 (Fig. 9E). The  $\alpha$ SMA gene expression reduced even when the ligation was released after one day and remained at a very low level until 21 days (Fig. 9E). Laminin 5 expression could not recover to a normal stage even when the suture was released after one day of ligation and showed punctate staining if the release was performed after seven days (Fig. 9B). Vimentin staining did not show an obvious difference between the ligation group and the release group, although fluorescence intensity analysis showed higher expression in the release group at day five and day seven (Supplementary Fig. S2).

## DISCUSSION

In this study, we blocked the rat lacrimal gland ducts for different durations up to three weeks to observe the pathological changes of the lacrimal gland. Moreover, we investigated the reversibility of lacrimal gland damage after ligation release at different time points. We found that the tear secretion was reduced to about half of the normal level after the ducts were ligated. Because only the duct of the exorbital lacrimal gland was ligated in our experiment, the infraorbital lacrimal gland may still produce tears to the ocular surface. However, such decrease of aqueous tear already resulted in corneal neovascularization in 25% to 35% of the animals, indicating that adequate tear is critical for maintaining homeostasis of the ocular surface.

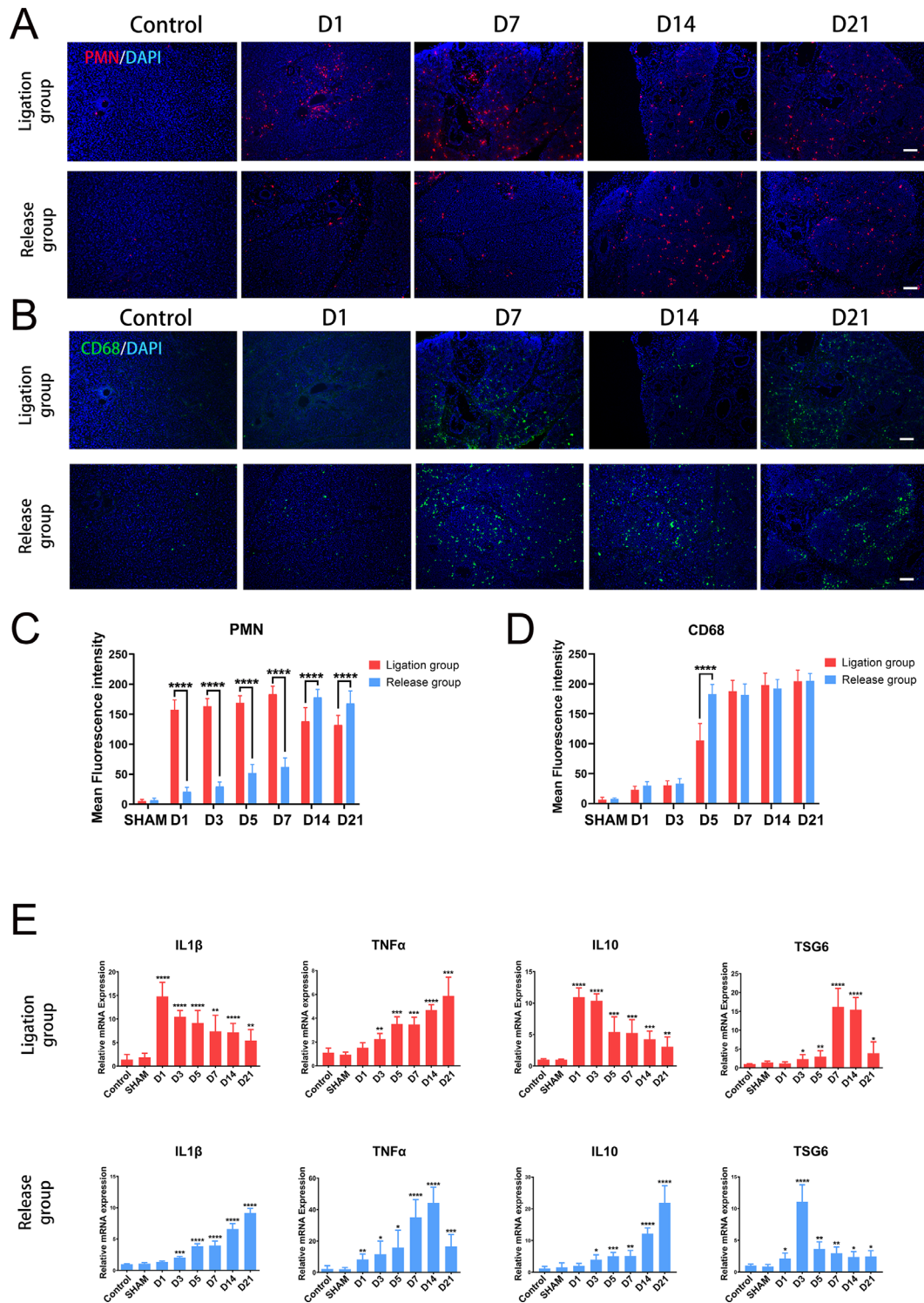


**FIGURE 7.** Inflammatory cell infiltration in the lacrimal gland after lacrimal duct blockage. (A) PMN staining showed that polymorphonuclear leukocyte infiltration into the lacrimal gland tissues was increased after one day in the ligation group and reduced before 14 days in the release group (Red: PMN; Blue: DAPI). Scale bar: 200 μm. (B) CD68 staining showed that macrophages infiltrating into the lacrimal gland increased after seven days in the ligation group and the release group (Green: CD68; Blue: DAPI). Scale bar: 200 μm. (C) Graph shows mean immunofluorescent intensity of PMN staining. (D) Graph shows mean immunofluorescent intensity of CD68 staining. (E) The qRT-PCR results show expression of IL1β, TNFα, IL10, and TSG6 of the lacrimal gland (n = 5; \*P < 0.5, \*\*P < 0.01, \*\*\*P < 0.001, \*\*\*\*P < 0.0001). The experiment was statistically analyzed using the one-way ANOVA test method (C, D). The experiment was statistically analyzed using the t test method (E).

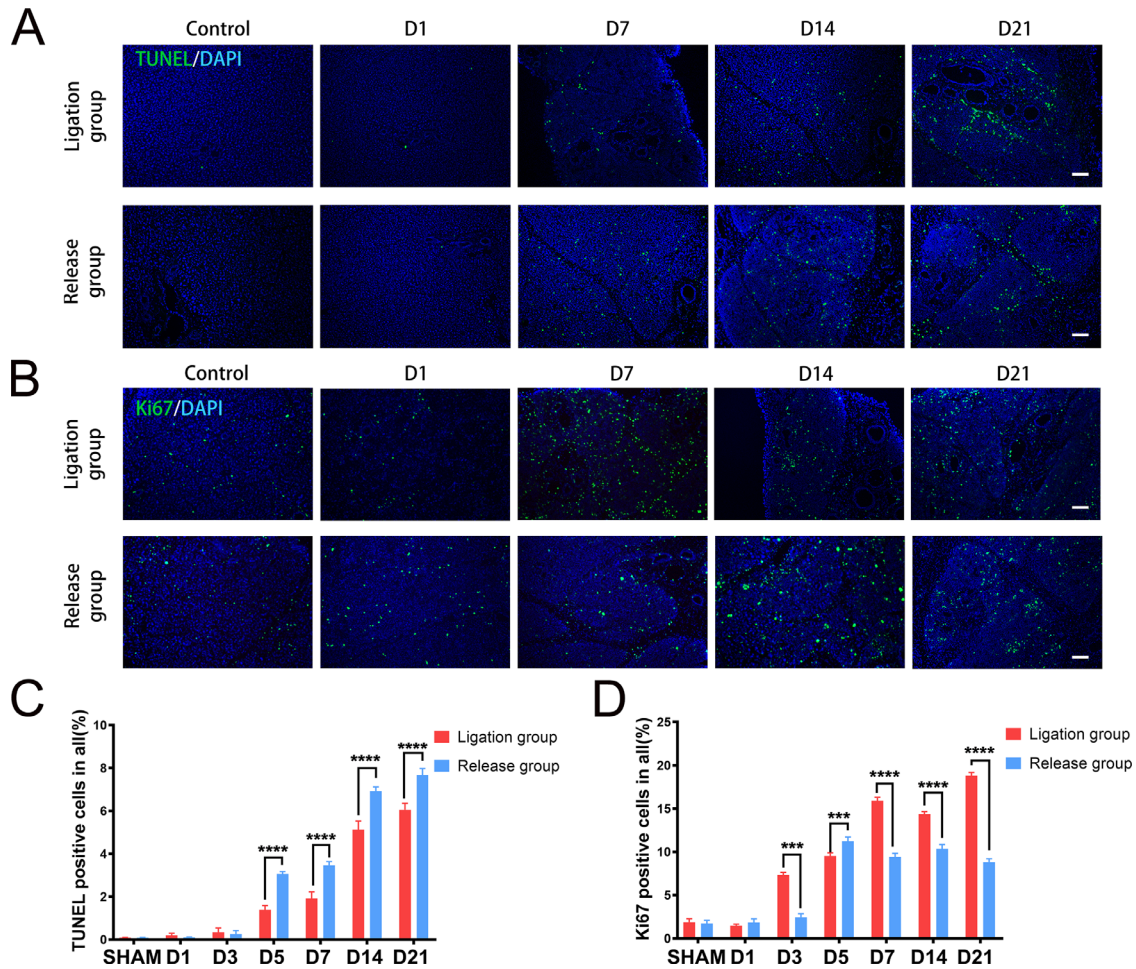


**FIGURE 8.** Cell proliferation and apoptosis in lacrimal gland after obstruction of lacrimal gland ducts. (A) TUNEL staining shows that apoptotic cells in the lacrimal gland increased after seven days in the ligation group and the release group (Green: TUNEL; Blue: DAPI). Scale bar: 200  $\mu$ m. (B) Immunofluorescence staining of Ki67 shows that proliferative cells in the lacrimal gland increase after seven days in the ligation group and the release group (Green: Ki67; Blue: DAPI). Scale bar: 200  $\mu$ m. (C) Graphs show the quantification of TUNEL positive cells in the lacrimal gland. (D) Graphs show quantification of Ki67-positive cells in the lacrimal gland ( $n = 5$ ; \*\*\*\* $P < 0.001$ ). The experiment was statistically analyzed using the one-way ANOVA test method (C, D).

In this study, the damage to the lacrimal gland mainly originated from ductal obstruction. However, ischemia caused by obstruction of some small vessels could not be ruled out. We ligated all ducts of the lacrimal gland, as well as small vessels that were difficult to separate from each other, accompanied by ducts during construction of the model. Obstruction of these small blood vessels may have some effect on the lacrimal gland.<sup>23,24</sup> This may not be identical to the pathological changes of simple lacrimal duct outlet occlusion in clinical practice.

After the sutures were released, the tear secretion could be recovered if the sutures were released before 14 days, although it could not recover to normal level if the ligation were prolonged to 21 days. AQP5 plays an important role in maintaining lacrimal gland homeostasis and tear secretion and will lead to the development of dry eye when AQP5 is deficient.<sup>25,26</sup> We found that short-term duct obstruction promoted AQP5 expression at the acinar apex, but long-term obstruction resulted in irreversible reduction of AQP5. The nerve is also essential in maintaining the normal secretory function of the lacrimal gland.<sup>27</sup> We also found that prolonged duct obstruction resulted in irreversible reduc-

tion of the lacrimal nerve. This supports the notion that there could be permanent lacrimal gland damage and function loss after long-term lacrimal duct obstruction. Because of obstruction of the ducts, the weight of the lacrimal gland slightly increased after one day. This may be attributed to edema of the acinus. However, the weight of lacrimal gland gradually declined after seven days ligation and reached about only 30% of the normal control after 21 days ligation. Although the blockage was released, the weight of lacrimal gland could not recover to normal stage if the ligation was released after five days. Although it was reported that the lacrimal gland has a powerful regenerative capacity after inflammation or injury,<sup>28</sup> our results suggest that long-term ligation induces irreversible atrophy of the lacrimal gland within 21 days. Whether a longer period can allow lacrimal gland injury to repair still needs more exploration in future study.

H&E staining and Masson staining further confirmed histological changes of the lacrimal glands after duct ligation. First, major ducts of the lacrimal gland dilated, and many new small ducts emerged after three days' ligation and became prominent as ligation prolonged. This may

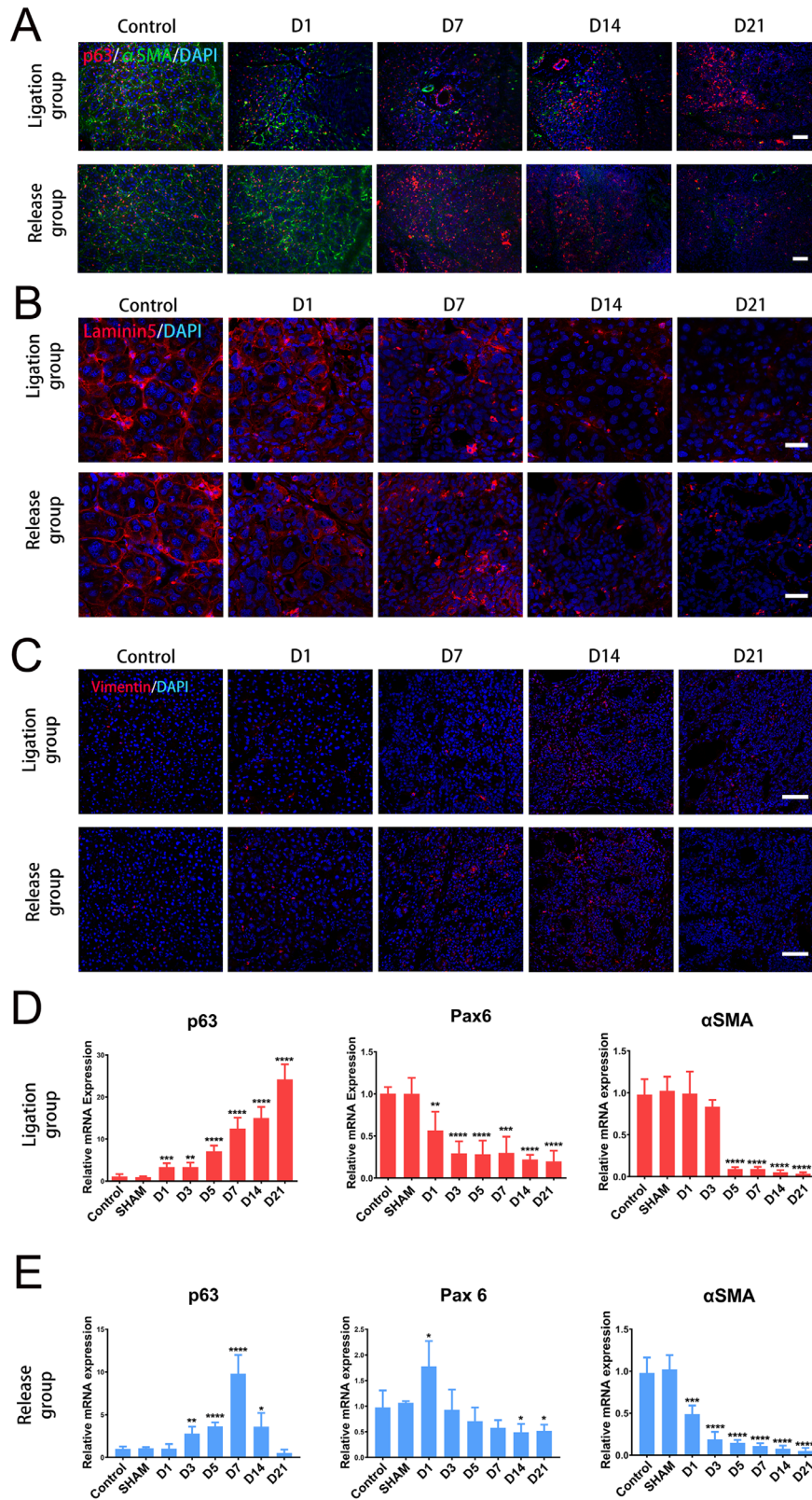


**FIGURE 9.** Lacrimal gland progenitor cell and basement membrane changes after obstruction of lacrimal gland ducts. (A) Images show immunofluorescence staining of p63-positive cells and myoepithelial cells in the lacrimal gland (Green: αSMA; Red: p63; Blue: DAPI). Scale bar: 200 μm (B) Immunofluorescence staining of laminin 5 shows basement membrane changes in the lacrimal gland (Red: Laminin 5; Blue: DAPI). Scale bar: 20 μm. (C) Immunofluorescence staining of Vimentin reveals that mesenchymal cells in the lacrimal gland increased after seven days and reduced after 21 days (Red: Vimentin; Blue: DAPI). Scale bar: 40 μm. (D) The qRT-PCR results show the expression of p63, Pax6, and αSMA in the lacrimal gland of the ligation group. (E) The qRT-PCR results show the expression of p63, Pax6, and αSMA in the lacrimal gland of the release group (n = 5; \*P < 0.5, \*\*P < 0.01, \*\*\*P < 0.001, \*\*\*\*P < 0.001). The experiment was statistically analyzed using the *t* test method (D, E).

be due to the retrograde intraduct pressure increase that resulted from duct ligation. Similar pathological change was found in the kidney where there is a blockage of the ureter by ureteral calculus or cancer.<sup>29</sup> Besides, ductal obstruction of the salivary glands also initiates inflammation and fibrosis of the tissues.<sup>30,31</sup> Prolonged drain duct blockage eventually induced atrophy of the acinus, along with fibrosis that surrounded the major ducts. Blocking of the ducts also induced inflammation of the lacrimal glands, as evidenced by infiltration of PMN and macrophages, and upregulated expression of inflammatory cytokines such as IL-1 $\beta$  and TNF $\alpha$ . Inflammation is involved in many lacrimal gland diseases, such as high-fat diet-related dry eye, autoimmune disease-related dry eye, and graft-versus-host disease-related dry eye.<sup>32–34</sup> Lacrimal duct blockage-induced inflammation may also contribute to acinar cell apoptosis and fibrosis.

Second, we found that lacrimal duct obstruction could lead to lipid accumulation. Our recent studies demonstrated that a high-fat diet and sleep deprivation could induce abnormal lipid accumulation in the lacrimal gland,<sup>34,35</sup> result in oxidative stress and inflammation, and further induce lacrimal gland damage such as acinus apoptosis and myoepithelial damage. The pattern of lipid deposition in a high-fat diet or sleep deprivation model was diffused in acini cells and in extracellular matrix, although it showed as patches in a current lacrimal duct ligation model. Different lipid deposition patterns may result from different pathogenesis. Duct ligation could cause intraduct hypertension and induce retrograde acinar dysfunction; therefore the first-line affected acini may be close to the major ducts. Similar changes were reported in the kidney and were the result of nephric duct obstruction.<sup>36,37</sup> Obstruction of the duct also causes fibrosis, glandular atrophy, and ductal dilation of the pancreas and liver.<sup>38</sup> On the other hand, high-fat diet- and sleep deprivation-induced pathological changes originated from blood circulation and thus may affect all the acinar cells, resulting in diffused lipid deposition.

Third, ligation of the lacrimal ducts led to significant downregulation of  $\alpha$ SMA of myoepithelial cells. It is known that contraction of myoepithelial cells helps tear production.<sup>39</sup> Several studies have suggested that myoepithelial cells play an important role in lacrimal gland repair and homeostasis.<sup>10,39</sup> There are also studies suggesting that myoepithelial cells are the progenitor of lacrimal gland acinar cells.<sup>22,39</sup> We found that  $\alpha$ SMA is very sensitive to duct ligation. The mRNA and protein expression of  $\alpha$ SMA dramatically reduced after five days' ligation. In the release group, even one day of ligation resulted in significant decrease of  $\alpha$ SMA after 21 days' observation time, and there was no recovery from day three to day 21. Future studies may apply this model to further investigate pathophysiology of myoepithelial cells and determine the function of myoepithelial cells during lacrimal gland wound healing.

The  $\Delta$ Np63 and Pax6 are expressed in myoepithelial cells and acinar cells of lacrimal gland. They play an important role in maintaining the function and development of the lacrimal gland.<sup>22,40</sup> Our data showed that p63 mRNA expression was upregulated and  $\Delta$ Np63 positive cells increased after duct ligation from day one to day 21, which is in accord with Ki67 expression. Although proliferating cells increased, there was also an increase of apoptotic cells. Moreover, the expanded cells did not form normal acinar structure and lost Pax6, indicating that they lack a normal phenotype and thus may not function normally. This may explain why the tear

secretion did not recover to a normal level after 21 days' ligation or release ligation for 21 days.

It was found that there were stem cells in the normal lacrimal gland, and the number of stem cells increased during the repair of lacrimal gland injury.<sup>16</sup> It has been found that injection of mesenchymal stem cells or mesenchymal stem cell secretomes can help lacrimal gland regeneration.<sup>41,42</sup> In the current study, the number of mesenchymal cells increased in response to two weeks of stimulation with lacrimal duct obstruction. However, longer-term duct obstruction will lead to a decrease in the number of vimentin-positive cells, and it is speculated that the imbalance of lacrimal gland homeostasis at this time leads to cell differentiation or death. At seven days of suture release, we saw an increase of vimentin, indicating that mesenchymal cells may be involved in the damage repair process of the lacrimal gland at this time. Although long-term lacrimal duct obstruction leads to an irreversible reduction in mesenchymal cell. More studies are needed to investigate the involvement of mesenchymal stem cells in this model in the future.

Interactions between epithelial cells and basement membrane regulate epithelial cell migration, proliferation, adhesion and differentiation.<sup>43</sup> Laminin 5 is expressed in the basement membrane of stratified and transitional epithelium. Deficiency or abnormality of laminin 5 could induce cicatricial pemphigoid.<sup>44</sup> Suppression of laminin 5 expression in mammary epithelial cells leads to the loss of reconstituted extracellular matrix-mediated growth control and apoptosis.<sup>45</sup> Also, it is a key factor in the differentiation of corneal epithelial progenitor cells and mesenchymal stem cells.<sup>46,47</sup> Here, we found that a basement membrane represented by laminin 5 is disrupted after duct obstruction, implying an imbalance in the microenvironment homeostasis of lacrimal gland epithelial cells, which may further affect the phenotype and function of lacrimal gland acinar cells. In the release group, the expression of laminin 5 could not recover to a normal level even there was only one day of ligation, indicating the basement membrane of the lacrimal gland acini is fragile and relatively difficult to regenerate after damage. The relationship between lacrimal gland wound healing and its basement membrane still needs further exploration.

In conclusion, blockage of lacrimal gland ducts may result in dystrophy of lacrimal gland acini, inflammation, and lipid accumulation of the lacrimal gland microenvironment. Long-term duct blockage will cause irreversible lacrimal gland failure. The prompt intervention of lacrimal gland duct obstruction is essential for the restoration of a functional lacrimal gland unit and to improve the prognosis of related diseases such as chemical burns, Stevens-Johnson syndrome, and mucous membrane pemphigoid.

### Acknowledgments

Supported in part by the National Key R&D Program of China (2018YFA0107301 [to W.L.], 2018YFA0107304 [to Z.L.]), the National Natural Science Foundation of China (NSFC, No. 81970773, No. 81770894 [to W.L.], No. 81870627 [to Z.L.]), and the Scientific Research Fund of The First Affiliated Hospital of Xiamen University (No. XYY2017011 [to Y.S.]).

Disclosure: **X. He**, None; **S. Wang**, None; **H. Sun**, None; **H. He**, None; **Y. Shi**, None; **Y. Wu**, None; **H. Wu**, None; **Z. Liu**, None; **J. Zhuang**, None; **W. Li**, None

## References

- Tsai P, Evans J, Green K, et al. Proteomic analysis of human meibomian gland secretions. *Br J Ophthalmol*. 2006;90:372–377.
- Mathers WD. Why the eye becomes dry: a cornea and lacrimal gland feedback model. *CLAO J*. 2000;26:159–165.
- Walcott B. The lacrimal gland and its veil of tears. *Physiology*. 1998;13:97–103.
- Obata H. Anatomy and histopathology of the human lacrimal gland. *Cornea*. 2006;25:S82–89.
- Shinomiya K, Ueta M, Kinoshita S. A new dry eye mouse model produced by exorbital and intraorbital lacrimal gland excision. *Sci Rep*. 2018;8:1483.
- Lorber M. Regional differences within the external 'duct' of the rat exorbital lacrimal gland. *Exp Eye Res*. 1993;56:471–480.
- Saika S, Kobata S, Hashizume N, Okada Y, Yamanaka O. Epithelial basement membrane in alkali-burned corneas in rats: immunohistochemical study. *Cornea*. 1993;12:383–390.
- Saika S, Uenoyama K, Hiroi K, Tanioka H, Takase K, Hikita M. Ascorbic acid phosphate ester and wound healing in rabbit corneal alkali burns: epithelial basement membrane and stroma. *Graefes Arch Clin Exp Ophthalmol*. 1993;231:221–227.
- Liu Y, Hirayama M, Kawakita T, Tsubota K. A ligation of the lacrimal excretory duct in mouse induces lacrimal gland inflammation with proliferative cells. *Stem Cells Int*. 2017;2017:4923426.
- Zoukhri D, Fix A, Alroy J, Kublin CL. Mechanisms of murine lacrimal gland repair after experimentally induced inflammation. *Invest Ophthalmol Vis Sci*. 2008;49:4399–4406.
- Burford-Mason AP, Cummins MM, Brown DH, MacKay AJ, Dardick I. Immunohistochemical analysis of the proliferative capacity of duct and acinar cells during ligation-induced atrophy and subsequent regeneration of rat parotid gland. *J Oral Pathol Med*. 1993;22:440–446.
- Takahashi S, Nakamura S, Suzuki R, et al. Apoptosis and mitosis of parenchymal cells in the duct-ligated rat submandibular gland. *Tissue Cell*. 2000;32:457–463.
- Takahashi S, Shinzato K, Nakamura S, Domon T, Yamamoto T, Wakita M. Cell death and cell proliferation in the regeneration of atrophied rat submandibular glands after duct ligation. *J Oral Pathol Med*. 2004;33:23–29.
- Walker NI, Gobé GC. Cell death and cell proliferation during atrophy of the rat parotid gland induced by duct obstruction. *J Pathol*. 1987;153:333–344.
- Lin H, Liu Y, He H, Botsford B, Yiu S. Lacrimal gland repair after short-term obstruction of excretory duct in rabbits. *Sci Rep*. 2017;7:8290.
- Dietrich J, Schlegel C, Roth M, et al. Comparative analysis on the dynamic of lacrimal gland damage and regeneration after Interleukin-1 $\alpha$  or duct ligation induced dry eye disease in mice. *Exp Eye Res*. 2018;172:66–77.
- Wang YC, Li S, Chen X, et al. Meibomian gland absence related dry eye in ectodysplasin a mutant mice. *Am J Pathol*. 2016;186:32–42.
- Ishida N, Hirai SI, Mita S. Immunolocalization of aquaporin homologs in mouse lacrimal glands. *Biochem Biophys Res Commun*. 1997;238:891–895.
- Ding C, Nandoskar P, Lu M, Thomas P, Trousdale MD, Wang Y. Changes of aquaporins in the lacrimal glands of a rabbit model of Sjögren's syndrome. *Curr Eye Res*. 2011;36:571–578.
- Jin K, Imada T, Hisamura R, et al. Identification of lacrimal gland postganglionic innervation and its regulation of tear secretion. *Am J Pathol*. 2020;190:1068–1079.
- de Souza RG, Yu Z, Hernandez H, et al. Modulation of oxidative stress and inflammation in the aged lacrimal gland. *Am J Pathol*. 2021;191:294–308.
- Shatos MA, Haugaard-Kedstrom L, Hodges RR, Dartt DA. Isolation and characterization of progenitor cells in uninjured, adult rat lacrimal gland. *Invest Ophthalmol Vis Sci*. 2012;53:2749–2759.
- Luibil N, Lopez MJ, Patel BC. Anatomy, head and neck, orbit. *StatPearls* [Internet]. Available from: <https://www.ncbi.nlm.nih.gov/books/NBK539843/>.
- Ducasse A, Delattre JF, Flament JB, Hureau J. The arteries of the lacrimal gland. *Anat Clin*. 1984;6:287–293.
- Hu S, Di G, Cao X, et al. Lacrimal gland homeostasis is maintained by the AQP5 pathway by attenuating endoplasmic reticulum stress inflammation in the lacrimal gland of AQP5 knockout mice. *Mol Vis*. 2021;27:679–690.
- Liu Y, Di G, Hu S, et al. Expression profiles of CircRNA and mRNA in lacrimal glands of AQP5(-/-) mice with primary dry eye. *Front Physiol*. 2020;11:1010.
- Dartt DA. Neural regulation of lacrimal gland secretory processes: relevance in dry eye diseases. *Prog Retin Eye Res*. 2009;28:155–177.
- Kawakita T. Regeneration of lacrimal gland function to maintain the health of the ocular surface. *Invest Ophthalmol Vis Sci*. 2018;59:Des169–des173.
- Tabib C, Nethala D, Kozel Z, Okeke Z. Management and treatment options when facing malignant ureteral obstruction. *Int J Urol*. 2020;27:591–598.
- Woods LT, Camden JM, El-Sayed FG, et al. Increased expression of TGF- $\beta$  signaling components in a mouse model of fibrosis induced by submandibular gland duct ligation. *PLoS One*. 2015;10:e0123641.
- Correia PN, Carpenter GH, Osailan SM, Paterson KL, Proctor GB. Acute salivary gland hypofunction in the duct ligation model in the absence of inflammation. *Oral Dis*. 2008;14:520–528.
- Rao P, McKown RL, Laurie GW, Suvas S. Development of lacrimal gland inflammation in the mouse model of herpes stromal keratitis. *Exp Eye Res*. 2019;184:101–106.
- Zoukhri D. Effect of inflammation on lacrimal gland function. *Exp Eye Res*. 2006;82:885–898.
- He X, Zhao Z, Wang S, et al. High-fat diet-induced functional and pathologic changes in lacrimal gland. *Am J Pathol*. 2020;190:2387–2402.
- Li S, Ning K, Zhou J, et al. Sleep deprivation disrupts the lacrimal system and induces dry eye disease. *Exp Mol Med*. 2018;50:e451.
- Higgins DF, Lappin DW, Kieran NE, et al. DNA oligonucleotide microarray technology identifies fisp-12 among other potential fibrogenic genes following murine unilateral ureteral obstruction (UUO): modulation during epithelial-mesenchymal transition. *Kidney Int*. 2003;64:2079–2091.
- Higgins DF, Kimura K, Bernhardt WM, et al. Hypoxia promotes fibrogenesis in vivo via HIF-1 stimulation of epithelial-to-mesenchymal transition. *J Clin Invest*. 2007;117:3810–3820.
- Panozzo MP, Basso D, Plebani M, Valente ML, Rasia E, Balint L. Effects of pancreaticobiliary duct obstruction on the exocrine and endocrine rat pancreas. *Pancreas*. 1995;11:408–414.
- Makarenkova HP, Dartt DA. Myoepithelial cells: their origin and function in lacrimal gland morphogenesis, homeostasis, and repair. *Curr Mol Biol Rep*. 2015;1:115–123.
- Ackermann P, Hetz S, Dieckow J, et al. Isolation and investigation of presumptive murine lacrimal gland stem cells. *Invest Ophthalmol Vis Sci*. 2015;56:4350–4363.

41. Dietrich J, Ott L, Roth M, et al. MSC Transplantation Improves Lacrimal Gland Regeneration after Surgically Induced Dry Eye Disease in Mice. *Sci Rep.* 2019;9:18299.
42. Dietrich J, Roth M, König S, Geerling G, Mertsch S, Schrader S. Analysis of lacrimal gland derived mesenchymal stem cell secretome and its impact on epithelial cell survival. *Stem Cell Res.* 2019;38:101477.
43. Ekblom M, Falk M, Salmivirta K, Durbeej M, Ekblom P. Laminin isoforms and epithelial development. *Ann NY Acad Sci.* 1998;857:194–211.
44. Kirtschig G, Marinkovich MP, Burgeson RE, Yancey KB. Anti-basement membrane autoantibodies in patients with anti-epiligrin cicatricial pemphigoid bind the alpha subunit of laminin 5. *J Invest Dermatol.* 1995;105:543–548.
45. Dietze EC, Bowie ML, Mrózek K, et al. CREB-binding protein regulates apoptosis and growth of HMECs grown in reconstituted ECM via laminin-5. *J Cell Sci.* 2005;118:5005–5022.
46. Yokoo S, Yamagami S, Shimada T, et al. A novel isolation technique of progenitor cells in human corneal epithelium using non-tissue culture dishes. *Stem Cells.* 2008;26:1743–1748.
47. Hashimoto J, Kariya Y, Miyazaki K. Regulation of proliferation and chondrogenic differentiation of human mesenchymal stem cells by laminin-5 (laminin-332). *Stem Cells.* 2006;24:2346–2354.